

Quantum magnets on the honeycomb and triangular lattices at $T = 0$

J. Oitmaa, C.J. Hamer, and Zheng Weihong

School of Physics, The University of New South Wales, P.O. Box 1, Kensington, New South Wales 2033, Australia

(Received 9 May 1991; revised manuscript received 6 November 1991)

We use series expansions around the Ising limit to study several anisotropic quantum spin models on the honeycomb and triangular lattices. These include the antiferromagnetic spin- $\frac{1}{2}$ and spin-1 Heisenberg model, and the XY antiferromagnet on the honeycomb lattice, and also the XY ferromagnet on the triangular lattice. Series are calculated for the ground-state energy, energy gap, magnetization, and magnetic susceptibility in each spin direction. Extrapolating these series to the isotropic limit, we find quite good agreement with the predictions of spin-wave theory.

The discovery of high- T_c superconductivity in materials containing two-dimensional Cu-O planes has generated a surge of interest in the Heisenberg antiferromagnet in two dimensions.¹ Recently, we have carried out series expansions^{2,3} around the Ising limit and a second-order spin-wave analysis⁴ for the Heisenberg antiferromagnet on a square lattice and found the spin-wave predictions to be in extremely good agreement with the results of series estimates.

Other lattices are also of interest. Recently a Monte Carlo (MC) simulation⁵ and a spin-wave calculation⁴ have indicated that quantum fluctuations for the Heisenberg antiferromagnet on the honeycomb lattice are much stronger than on the square lattice, but the system still possesses Néel order.

The XY model has many features in common with the Heisenberg antiferromagnet: it has recently been reviewed by Betts and Miyashita.⁶ Oitmaa and Betts⁷ estimated the ground-state energy of the XY model on the

honeycomb lattice, using finite-cell methods. Previous work on the XY ferromagnet on the triangular lattice includes the finite-cell calculations of Marland and Betts⁸ and of Fujiki and Betts.⁹

This paper presents the results of series expansions about the Ising limit for the zero-temperature Heisenberg antiferromagnet and XY model on the honeycomb lattice and the XY ferromagnet on the triangular lattice, together with an analysis based upon series. It forms a companion paper to a similar study of the square-lattice Heisenberg antiferromagnet and XY model, which we recently carried out.^{2,3} The notations here have the same meaning as in these previous papers.

To calculate the series, we used Nickel's cluster-expansion method,¹⁰ which has been discussed and extended by Marland,¹¹ Irving and Hamer,¹² and Hamer and Irving.¹³ The techniques necessary were reviewed recently in He, Hamer, and Oitmaa¹⁴ and will not be

TABLE I. Series coefficients for the ground-state energy per site E_0/N , the staggered magnetization M^+ , staggered parallel susceptibility χ_{\parallel}^S , and the energy gap m . Coefficients of x^n are listed for both the spin- $\frac{1}{2}$ and spin-1 Heisenberg antiferromagnets.

n	E_0/N	M^+	χ_{\parallel}^S	m
Spin- $\frac{1}{2}$ XXZ model				
0	-3/8	1/2	0	3/2
2	-3/16	-3/16	3/8	-15/8
4	$0.273437500000 \times 10^{-1}$	$0.403645833333 \times 10^{-1}$	$0.329861111111 \times 10^{-1}$	$0.230468750000 \times 10^1$
6	$-0.126139322917 \times 10^{-1}$	$-0.521240234375 \times 10^{-1}$	0.349116572627	$-0.705102539062 \times 10^1$
8	$0.707260885356 \times 10^{-2}$	$0.363588183996 \times 10^{-1}$	-0.183672262247	$0.263766856347 \times 10^2$
10	$-0.633543855761 \times 10^{-2}$	$-0.549560908381 \times 10^{-1}$	0.621001303118	$-0.111596182008 \times 10^3$
12	$0.572416455774 \times 10^{-2}$	$0.587184537380 \times 10^{-1}$	-0.667550589179	
14	$-0.596881924367 \times 10^{-2}$	$-0.789585827735 \times 10^{-1}$	$0.123052125571 \times 10^1$	
Spin-1 XXZ model				
0	-3/2	1	0	3
2	-3/10	-3/25	12/125	-39/20
4	$-0.181666666667 \times 10^{-1}$	$-0.332907407407 \times 10^{-1}$	$0.734217695473 \times 10^{-1}$	-0.214601190476
6	$-0.431102391436 \times 10^{-2}$	$-0.138307230561 \times 10^{-1}$	$0.507964233362 \times 10^{-1}$	-0.111765872310
8	$-0.272844564317 \times 10^{-2}$	$-0.109725035060 \times 10^{-1}$	$0.508208807023 \times 10^{-1}$	-0.129172108748
10	$-0.127998263541 \times 10^{-2}$	$-0.716412836371 \times 10^{-2}$	$0.438943164418 \times 10^{-1}$	$-0.287788748355 \times 10^{-1}$
12	$-0.817014232889 \times 10^{-3}$	$-0.550075655175 \times 10^{-2}$	$0.404687373995 \times 10^{-1}$	

TABLE II. Series coefficients for the perpendicular susceptibility χ_{\perp} . Coefficients of x^n are listed for both the spin- $\frac{1}{2}$ and spin-1 Heisenberg antiferromagnets.

n	Spin- $\frac{1}{2}$	Spin-1
0	1/3	1/3
1	-1/2	-2/5
2	0.566666666667	0.409523809524
3	-0.590277777778	-0.429132275132
4	0.595833333333	0.433224824206
5	-0.637851060563	-0.439821667828
6	0.649541367026	0.441281954982
7	-0.625790891852	-0.446894480327
8	0.622500161232	0.448328489653
9	-0.679789419424	-0.451717439927
10	0.692650685491	0.452477386182
11	-0.627079462804	
12	0.623731925514	
13	-0.725511320444	

repeated here. The major difference is that a “low-temperature” expansion is involved in the present case, requiring the calculation of “strong” embedding constants for the clusters involved.¹⁵

The Heisenberg antiferromagnet with anisotropy can be described by the following Hamiltonian:

$$H = \sum_{\langle lm \rangle} [S_l^z S_m^z + x(S_l^x S_m^x + S_l^y S_m^y)], \quad (1)$$

where $\langle lm \rangle$ denotes a sum over all nearest-neighbor

pairs. The limits $x = 0$ and $x = 1$ correspond to the antiferromagnetic Ising model and isotropic Heisenberg model, respectively. The series have been calculated for the ground state energy per site E_0/N , the energy gap m , the staggered magnetization M^+ , the parallel staggered susceptibility χ_{\parallel}^S , and the uniform perpendicular susceptibility χ_{\perp} . The staggered perpendicular susceptibility χ_{\perp}^S is related to χ_{\perp} by the relation $\chi_{\perp}^S(x) = \chi_{\perp}(-x)$.

The quantum XY model with anisotropy can be described by the following Hamiltonian:

$$H = - \sum_{\langle lm \rangle} (S_l^x S_m^x + x S_l^y S_m^y), \quad (2)$$

where the points $x = 0$ and $x = 1$ correspond to the ferromagnetic Ising model and isotropic ferromagnetic XY model (F), respectively. For bipartite lattice such as the honeycomb lattice, the isotropic antiferromagnetic XY model (A),

$$H^A = \sum_{\langle lm \rangle} (S_l^x S_m^x + S_l^y S_m^y), \quad (3)$$

is related to the ferromagnetic one by a simple spin transformation. Hence, there exist the following relations between the isotropic XY ferromagnet (F), antiferromagnet (A) and the model described by Eq. (2):

TABLE III. Series coefficients for the ground-state energy per site E_0/N , the magnetization M_x , and the parallel susceptibility χ_{xx} of spin- $\frac{1}{2}$ XY model. Coefficients of x^n are listed.

n	E_0/N	M_x	χ_{xx}
Spin- $\frac{1}{2}$ XY model on the honeycomb lattice			
0	-3/8	1/2	0
1	-3/64	-3/64	3/32
4	-0.219726562500 $\times 10^{-2}$	-0.789388020833 $\times 10^{-2}$	0.393880208333 $\times 10^{-1}$
6	-0.107243855794 $\times 10^{-2}$	-0.585550096300 $\times 10^{-2}$	0.403963481762 $\times 10^{-1}$
8	-0.379281057252 $\times 10^{-3}$	-0.310399798228 $\times 10^{-2}$	0.301486151342 $\times 10^{-1}$
10	-0.227691587386 $\times 10^{-3}$	-0.236391068449 $\times 10^{-2}$	0.283352420881 $\times 10^{-1}$
12	-0.131617242867 $\times 10^{-3}$	-0.170132238119 $\times 10^{-2}$	0.248037012945 $\times 10^{-1}$
14	-0.888694343778 $\times 10^{-4}$	-0.136039067101 $\times 10^{-2}$	0.231427460008 $\times 10^{-1}$
Spin- $\frac{1}{2}$ XY ferromagnet on the triangular lattice			
0	-3/4	1/2	0
1	0	0	0
2	-3.750000000000 $\times 10^{-2}$	-1.500000000000 $\times 10^{-2}$	1.200000000000 $\times 10^{-2}$
3	-7.500000000000 $\times 10^{-3}$	-6.000000000000 $\times 10^{-3}$	7.200000000000 $\times 10^{-3}$
4	-3.102678571429 $\times 10^{-3}$	-3.979804421769 $\times 10^{-3}$	6.881251349746 $\times 10^{-3}$
5	-1.557667824074 $\times 10^{-3}$	-2.712120351999 $\times 10^{-3}$	5.955784808394 $\times 10^{-3}$
6	-9.211778440233 $\times 10^{-4}$	-2.036015126868 $\times 10^{-3}$	5.458238255317 $\times 10^{-3}$
7	-5.949645601858 $\times 10^{-4}$	-1.595024933200 $\times 10^{-3}$	5.043787122963 $\times 10^{-3}$
8	-4.102048269505 $\times 10^{-4}$	-1.293661312397 $\times 10^{-3}$	4.715484327163 $\times 10^{-3}$
9	-2.965849752473 $\times 10^{-4}$	-1.076042759738 $\times 10^{-3}$	4.442176283847 $\times 10^{-3}$
10	-2.225228426269 $\times 10^{-4}$	-9.131920333434 $\times 10^{-4}$	4.211586729215 $\times 10^{-3}$
11	-1.719313540898 $\times 10^{-4}$	-7.875467446608 $\times 10^{-4}$	4.013342629066 $\times 10^{-3}$

$$\begin{aligned}
E_0(x=1) &= E_0(x=-1) = E_0^A = E_0^F, \\
M_x(x=1) &= M_x(x=-1) = M_x^F = M_x^{A,S}, \\
\chi_{xx}(x=1) &= \chi_{xx}(x=-1) = \chi_{xx}^F = \chi_{xx}^{A,S}, \\
\chi_{yy}(x=1) &= \chi_{yy}^{A,S} = \chi_{yy}^F, \\
\chi_{yy}(x=-1) &= \chi_{yy}^A = \chi_{yy}^{F,S}, \\
\chi_{zz}(x=1) &= \chi_{zz}^A = \chi_{zz}^F, \\
\chi_{zz}(x=-1) &= \chi_{zz}^{A,S} = \chi_{zz}^{F,S},
\end{aligned} \tag{4}$$

where the superscript S denotes the staggered magnetization and susceptibility.

The triangular lattice is not a bipartite lattice, and the ground-state energy E_0 , and its derivatives are functions of x , rather than functions of x^2 as in the case of bipartite lattices. Therefore, we can easily obtain effective longer series compared with those on the bipartite lattices.

The resulting series for the spin- $\frac{1}{2}$ and spin-1 Heisenberg antiferromagnet, spin- $\frac{1}{2}$ XY model on a honeycomb lattice, and the spin- $\frac{1}{2}$ XY ferromagnet on a triangular lattice are listed in Tables I–IV. The calculation of the

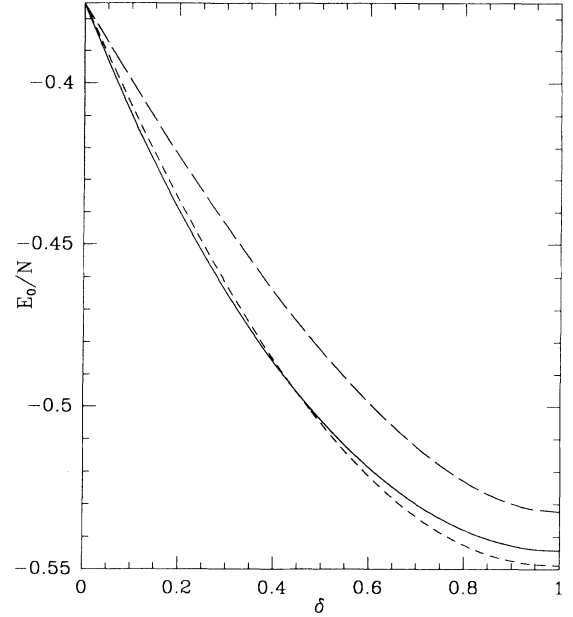


FIG. 1. Graph of the ground-state energy per site E_0/N against $\delta = 1 - (1 - x^2)^{1/2}$ for the spin- $\frac{1}{2}$ Heisenberg antiferromagnet on the honeycomb lattice. The three curves shown are the series estimate, and the first- and second-order spin-wave predictions, corresponding to solid, long-dashed and short-dashed lines, respectively.

TABLE IV. Series coefficients for the transverse susceptibility χ_{yy} , χ_{zz} , and the energy gap m of spin- $\frac{1}{2}$ XY model. Coefficients of x^n are listed.

n	χ_{yy}	χ_{zz}	m
Spin- $\frac{1}{2}$ XY model on the honeycomb lattice			
0	1/3	1/3	3/2
1	5/12	-1/12	-3/4
2	0.433333333333	$0.166666666667 \times 10^{-1}$	-0.468750000000
3	0.447395833333	$-0.572916666667 \times 10^{-2}$	0.187500000000
4	0.451324404762	$0.144841269841 \times 10^{-2}$	-0.184082031250
5	0.462027653401	$-0.135928753012 \times 10^{-2}$	$-0.536295572917 \times 10^{-1}$
6	0.464960119431	$0.289790709710 \times 10^{-3}$	0.102287038167
7	0.470034894435	$-0.369601665434 \times 10^{-3}$	-0.139394598714
8	0.471507036544	$0.438493259190 \times 10^{-4}$	$0.278560177338 \times 10^{-2}$
9	0.475584052742	$-0.170841551828 \times 10^{-3}$	$0.997611138995 \times 10^{-1}$
10	0.476865500686	$0.474438423932 \times 10^{-6}$	-0.186450762222
11	0.479664327048	$-0.744433257870 \times 10^{-4}$	
12	0.480600097830	$-0.109293285502 \times 10^{-4}$	
13	0.482868059374	$-0.424038822569 \times 10^{-4}$	
Spin- $\frac{1}{2}$ XY ferromagnet on the triangular lattice			
0	1/6	1/6	3
1	-1/60	11/60	-3/2
2	$7.142857142857 \times 10^{-4}$	$1.907142857143 \times 10^{-1}$	$-5.625000000000 \times 10^{-1}$
3	$-6.408730158730 \times 10^{-4}$	$1.946442743764 \times 10^{-1}$	$-1.275000000000 \times 10^{-1}$
4	$-1.800546199232 \times 10^{-4}$	$1.973205733120 \times 10^{-1}$	$-1.188066406250 \times 10^{-1}$
5	$-1.342299379565 \times 10^{-4}$	$1.992487719282 \times 10^{-1}$	$-6.786934964850 \times 10^{-2}$
6	$-8.198102604710 \times 10^{-5}$	$2.007544340145 \times 10^{-1}$	$-5.515799640553 \times 10^{-2}$
7	$-5.839468270410 \times 10^{-5}$	$2.019580934726 \times 10^{-1}$	$-4.117578477384 \times 10^{-2}$
8	$-4.218621969602 \times 10^{-5}$	$2.029518171697 \times 10^{-1}$	$-3.384263314391 \times 10^{-2}$
9	$-3.186501396235 \times 10^{-5}$	$2.037901728331 \times 10^{-1}$	$-2.807294719610 \times 10^{-2}$
10	$-2.469393761322 \times 10^{-5}$	$2.045101675703 \times 10^{-1}$	

ground state energy and its derivatives involved a list of 1223 linked clusters (up to 14 sites) for the honeycomb lattice, or 6634 linked clusters (up to 11 sites) for the triangular lattice, together with their lattice constants and embedding constants; the calculation of the energy gap required a further 638 clusters (up to 11 sites), or 3763

clusters (up to 10 sites), both linked and unlinked. The calculation took about 40 h on an IBM 3090.

The analysis of these series was carried out along the same lines as our previous papers^{2,3} and we will not repeat the details here. Firstly, we have endeavored, by use of D log Padé approximants and differential

TABLE V. Estimates of singularity parameters for the series given in Tables I–IV. Both unbiased estimates and estimates biased by setting $x_c^2 = 1$ are listed. The index values predicted by spin wave theory are also given for comparison.

Function	Singular point x_c^2	Singularity index		Spin-wave prediction
		Unbiased	Biased	
Spin- $\frac{1}{2}$ XXZ model on the honeycomb lattice				
m	0.9(4)	0.5(3)	0.56(15)	0.5
$\chi_{//}^S$	1.00(15)	-0.6(3)	-0.6(1)	-0.5
$\frac{dM^+}{dx^2}$	1.0(3)	-0.58(20)	-0.50(8)	-0.5
$\frac{d^2 E_0}{d(x^2)^2}$	0.85(30)			-0.5
$\frac{d\chi_{\perp}}{dx}$	$x_c = 1.04(20)$	-0.6(3) ^a	-0.48(4)	-0.5
χ_{\perp}^S	$x_c = 0.99(1)$	-1.06(10)	-1.07(7)	-1.0
Spin-1 XXZ model on the honeycomb lattice				
m	1.00(8)	0.55(10)	0.55(6)	0.5
$\chi_{//}^S$	1.06(10)	-0.8(4)	-0.65(10)	-0.5
$\frac{dM^+}{dx^2}$	1.0(1)	-0.6(2)	-0.55(6)	-0.5
$\frac{d^2 E_0}{d(x^2)^2}$	0.9(4)	-0.9(5)	-0.6(3)	-0.5
$\frac{d\chi_{\perp}}{dx}$	$x_c = 0.9(3)$	-0.3(3)	-0.4(2)	-0.5
χ_{\perp}^S	$x_c = 1.003(10)$	-1.07(8)	-1.05(5)	-1.0
Spin- $\frac{1}{2}$ XY model on the honeycomb lattice				
$\frac{dM_x}{dx^2}$	1.01(1)	-0.52(3)	-0.50(1)	-0.5
$\frac{d^2 E_0}{d(x^2)^2}$	1.0(2)			-0.5
χ_{xx}	1.02(3)	-0.58(6)	-0.53(3)	-0.5
m ($x > 0$)	$x_c = 1.01(3)$	0.6(1)	0.56(6)	0.5
χ_{yy} ($x > 0$)	$x_c = 1.001(2)$	-1.06(5)	-1.04(3)	-1.0
$\frac{d\chi_{yy}}{dx}$ ($x < 0$)	$x_c = -0.95(10)$	-0.25(20)	-0.4(1)	-0.5
$\frac{d^2 \chi_{zz}}{dx^2}$ ($x > 0$)	$x_c = 0.7(2)$		-0.9(6) ^a	-0.5
$\frac{d^2 \chi_{zz}}{dx^2}$ ($x < 0$)	$x_c = -1.2(4)$	-0.4(4)	-0.3(2)	-0.5
Spin- $\frac{1}{2}$ XY model on the triangular lattice				
$\frac{dM_x}{dx}$	1.01(3)	-0.55(10)	-0.50(5)	-0.5
$\frac{d^2 E_0}{dx^2}$	1.00(2)	-0.57(10)	-0.52(3)	-0.5
χ_{xx}	1.01(2)	-0.6(2)	-0.50(5)	-0.5
χ_{yy}	1.002(2)	-1.03(3)	-1.02(2)	-1.0
$\frac{d^2 \chi_{zz}}{dx^2}$	1.05(6)	-1.0(2) ^a	-0.7(3)	-0.5
$\frac{dm}{dx}$	0.99(2)	-0.4(1)	-0.47(7)	-0.5

^aAll estimates defective

approximants,¹⁶ to test whether the singularities of these functions at $x = \pm 1$ are of the form predicted by spin wave theory.⁴ The results, given in Table V, show that the singularities and the indices are by and large quite consistent with the predictions of spin-wave theory. For the XXZ and XY model on the honeycomb lattice, just as for the square lattice,^{2,3} we did not get very consistent results between the series estimates and spin-wave theory for the singularity of the ground-state energy series because the series is too short and the singularity is very weak. But for the XY ferromagnet on the triangular lattice, we have a longer series, and Table V does show that the singularity of the ground-state energy is of the form predicted by spin-wave theory.

Next, we assume the singularities are those predicted by spin-wave theory, and estimate, by using integrated differential approximants, the coefficients of the leading-order terms for each given function f in the asymptotic expansion near $x = \pm 1$ defined by

$$f(x^2) = \sum_{n=n_0}^{\infty} A_n(1-x^2)^{n/2} \quad (x^2 \sim 1) \quad (5)$$

or

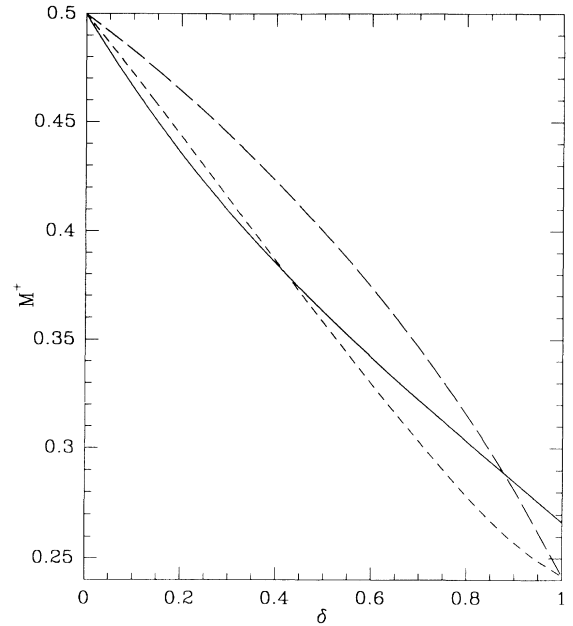


FIG. 2. Graph of the staggered magnetization M^+ against δ for the spin- $\frac{1}{2}$ Heisenberg antiferromagnet on the honeycomb lattice. Notation as in Fig. 1.

TABLE VI. Series estimates for the leading order amplitudes A_n of the spin- $\frac{1}{2}$ and spin-1 Heisenberg antiferromagnets at $x = 1$ [as defined by Eq. (5)]. Also listed are the spin-wave predictions at first and second order.

Function	n	Amplitudes A_n		Series Estimate
		Spin-wave predictions		
		First order	Second order	
Spin- $\frac{1}{2}$ XXZ model				
E_0/N	0	-0.5324	-0.5489	-0.5443(3)
	2	0.2723	0.1317	0.162(3)
	3	-0.2068	0.2003	-0.0134(10)
M^+	0	0.2418	0.2418	0.266(9)
	1	0.4135	0.1132	0.18(3)
χ_{\perp}	0	0.1667	0.0456	0.0756(10)
	1		0.1378	0.060(4)
m	1	1.5	0.725	0.80(8)
	2		1.240	0.3(2)
χ_{\parallel}^S	-1	0.2757	0.4180	0.466(10)
	0	-0.3595	-0.2840	-0.37(2)
$(1-x)\chi_{\perp}^S$	0	0.3333	0.5754	0.75(4)
	1		-0.2757	-0.38(6)
Spin-1 XXZ model				
E_0/N	0	-1.8148	-1.8313	-1.8278(8)
	2	0.5447	0.4040	0.42(1)
	3	-0.4135	-0.0065	-0.14(3)
M^+	0	0.7418	0.7418	0.748(3)
	1	0.4135	0.2634	0.28(2)
χ_{\perp}	0	0.1667	0.1061	0.115(5)
	1		0.0689	0.045(6)
m	1	3	2.2254	2.27(4)
	2		1.24	0.6(1)
χ_{\parallel}^S	-1	0.1378	0.1734	0.177(6)
	0	-0.1797	-0.1609	-0.15(2)
$(1-x)\chi_{\perp}^S$	0	0.3333	0.4544	0.49(1)
	1		-0.1378	-0.15(2)

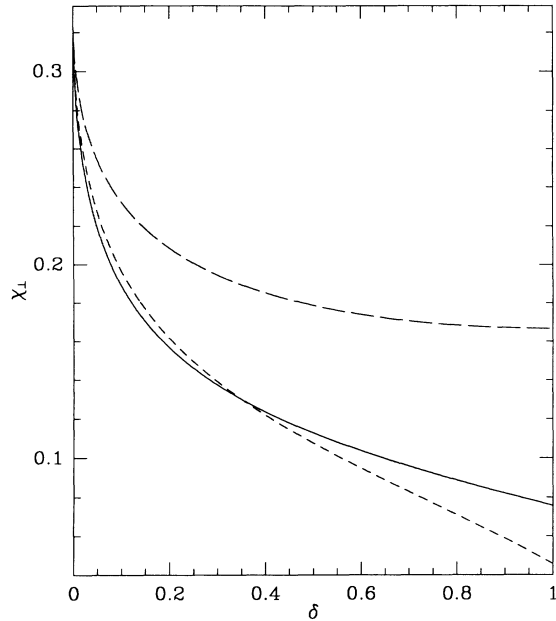


FIG. 3. Graph of the perpendicular susceptibility χ_{\perp} against δ for spin- $\frac{1}{2}$ Heisenberg antiferromagnet on the honeycomb lattice. Notation as in Fig. 1.

$$f(x) = \sum_{n=n_0}^{\infty} A_n (1 \mp x)^{n/2} \quad (x \sim \pm 1). \quad (6)$$

Our series estimates of these amplitudes A_n are listed in Tables VI–VIII, together with the predictions of spin-

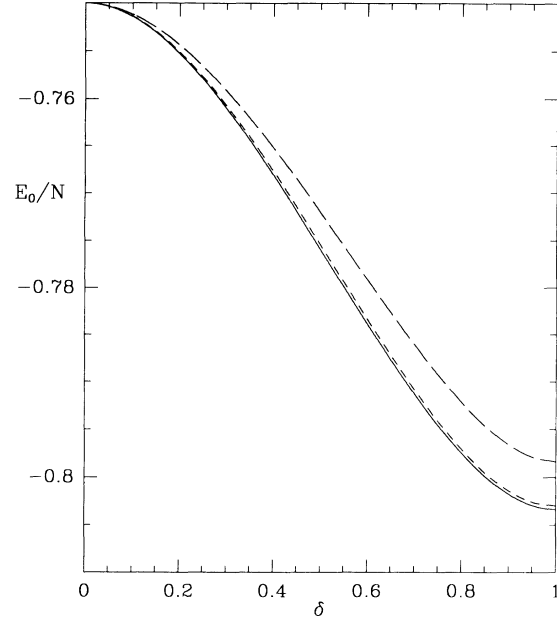


FIG. 4. Graph of the ground-state energy per site E_0/N against $\delta = 1 - (1 - x)^{1/2}$ for the spin- $\frac{1}{2}$ XY ferromagnet on the triangular lattice. Notation as in Fig. 1.

wave theory at first and second order in $1/S$.

The agreement between the spin-wave predictions and the series estimates is very good: the situation for the honeycomb lattice is not quite as good as in the case of the square lattice,^{2,3} but the situation for the triangular

TABLE VII. Series estimates for the leading order amplitudes A_n in asymptotic expansion at $x = \pm 1$ [defined by Eq. (5) or Eq. (6) as the case may be] of spin- $\frac{1}{2}$ XY model on the honeycomb lattice. Also listed are the spin-wave predictions at first and second order.

Function	x	n	Amplitudes A_n		Series Estimate
			Spin-wave predictions		
			First order	Second order	
E_0/N	± 1	0	-0.41672	-0.42440	-0.4261(1)
		2	0.080815	0.06127	0.0659(3)
		3	-0.0731	0.01054	-0.0225(8)
M_x	± 1	0	0.4201	0.4173	0.4133(3)
		1	0.14619	0.06530	0.084(2)
χ_{xx}	± 1	-1	0.09746	0.10113	0.104(4)
		0	-0.1555	-0.0225	-0.03(1)
m	1	1	1.5	1.0768	1.13(1)
		2		1.2405	0.50(5)
$(1-x)^{-1/2}m$	-1	0	1.5	1.4436	1.1(1)
		2		0.23155	0.9(4)
$(1-x)\chi_{yy}$	1	0	1/3	0.4770	0.522(4)
		1		-0.2757	-0.25(3)
χ_{yy}	-1	0	1/6	0.09483	0.1105(10)
		1		0.13783	0.040(4)
χ_{zz}	1	0	1/3	0.27118	0.26062(8)
		2		0.1029	0.0730(8)
χ_{zz}	-1	0	1/3	0.39548	0.44286(3)
		2		-0.1029	-0.1541(2)

TABLE VIII. Series estimates for the leading-order amplitudes A_n in the asymptotic expansion at $x = 1$ [defined by Eq. (6)] of the spin- $\frac{1}{2}$ XY ferromagnet on the triangular lattice. Also listed are the spin-wave predictions (Ref. 4) at first and second order.

Function	n	Amplitudes A_n		Series Estimate
		Spin-wave predictions		
		First order	Second order	
E_0/N	0	-0.79839	-0.80301	-0.8033(2)
	2	0.20278	0.1686	0.173(2)
	3	-0.27566	-0.0749	-0.136(6)
M_x	0	0.448533	0.448402	0.4483(3)
	1	0.1378	0.0889	0.095(4)
χ_{xx}	-1	0.02297	0.02339	0.0234(2)
	0	-0.05292	-0.02474	-0.029(1)
m	1	3	2.4374	2.485(3)
	2		1.654	0.93(2)
χ_{yy}	-2	1/6	0.21173	0.2191(2)
	-1		-0.0919	-0.085(2)
χ_{zz}	0	1/6	0.1498	0.14942(4)
	2		0.0310	0.022(1)

lattice is actually better. The agreement is further illustrated in Figs. 1–6, which graph the series estimates and spin-wave predictions as function of $\delta = 1 - (1 - x^2)^{1/2}$ for E_0/N , M_x and χ_{\perp} for the spin- $\frac{1}{2}$ Heisenberg antiferromagnet on the honeycomb lattice and XY ferromagnet on the triangular lattice.

For the Heisenberg antiferromagnet on the honeycomb lattice, the series estimates give the amplitude ratio R (defined in Ref. 2):

$$R(S = \frac{1}{2}) = 0.86(17),$$

$$R(S = 1) = 0.95(12),$$
(7)

which are in good agreement with the universality hypothesis.

For the spin- $\frac{1}{2}$ Heisenberg antiferromagnet on the honeycomb lattice, the staggered magnetization obtained

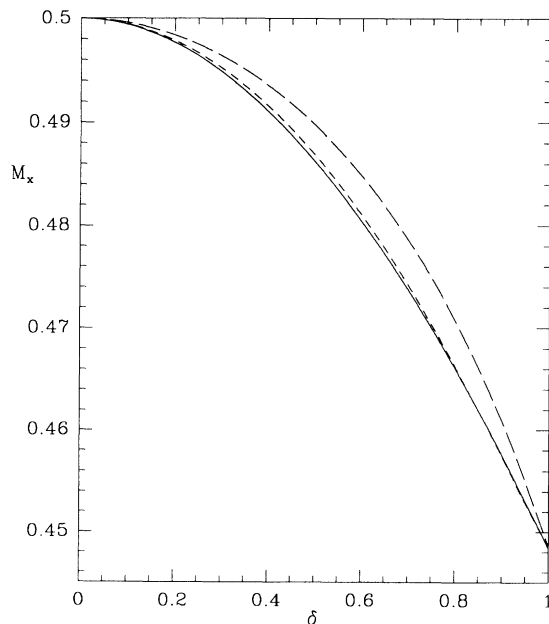


FIG. 5. Graph of the magnetization M_x against $\delta = 1 - (1 - x)^{1/2}$ for the spin- $\frac{1}{2}$ XY ferromagnet on the triangular lattice. Notation as in Fig. 1.

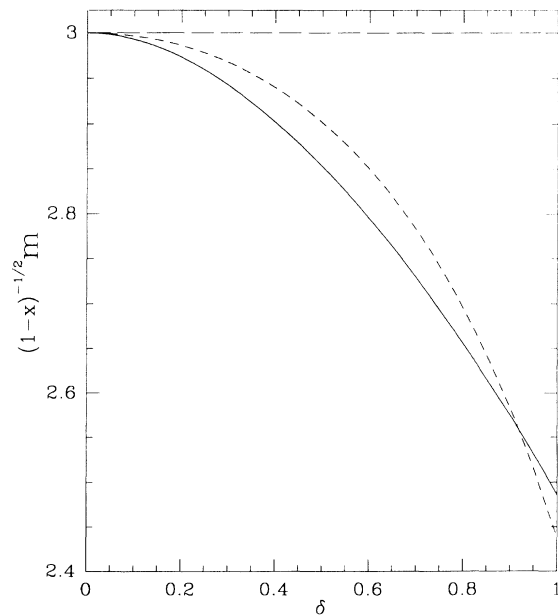


FIG. 6. Graph of the energy gap $(1 - x)^{-1/2}m$ against $\delta = 1 - (1 - x)^{1/2}$ for the spin- $\frac{1}{2}$ XY ferromagnet on the triangular lattice. Notation as in Fig. 1.

here is slightly larger than the spin wave prediction and the Monte Carlo estimates of Reger, Riera, and Young,⁵ who find $M^+ = 0.22(3)$ and $E_0/N = -0.5445(12)$. The zero-point spin reduction for the classical Néel state is larger than for the square lattice, indicating the stronger quantum fluctuations on the honeycomb lattice.

The ground-state energy per site for the XY ferromagnet on the triangular lattice obtained here is $E_0/N = -0.8033(2)$, which agrees with the finite lattice calcu-

lation by Fujiki and Betts⁹ who estimated $E_0/N = -0.7989(45)$, but our result is substantially more accurate.

ACKNOWLEDGMENT

This work forms parts of a research project supported by a grant from the Australian Research Council.

¹T. Barnes (unpublished).

²W.H. Zheng, J. Oitmaa, and C.J. Hamer, *Phys. Rev. B* **43**, 8321 (1991).

³C.J. Hamer, J. Oitmaa, and W.H. Zheng, *Phys. Rev. B* **43**, 10 789 (1991).

⁴W.H. Zheng, J. Oitmaa, and C.J. Hamer, *Phys. Rev. B* **44**, 11 869 (1991).

⁵J.D. Reger, J.A. Riera, and A.P. Young, *J. Phys. C* **1**, 1855 (1989).

⁶D.D. Betts and S. Miyashita, *Can. J. Phys.* (to be published), and references therein.

⁷J. Oitmaa and D.D. Betts, *Can. J. Phys.* **56**, 897 (1978).

⁸L.G. Marland and D.D. Betts, *Phys. Lett. A* **76**, 271 (1980).

⁹S. Fujiki and D.D. Betts, *Can. J. Phys.* **64**, 876 (1986).

¹⁰B.G. Nickel (unpublished).

¹¹L.G. Marland, *J. Phys. A* **14**, 2047 (1981).

¹²A.C. Irving and C.J. Hamer, *Nucl. Phys.* **B230**, 361 (1984).

¹³C.J. Hamer and A.C. Irving, *J. Phys. A* **17**, 1649 (1984).

¹⁴H.X. He, C.J. Hamer, and J. Oitmaa, *J. Phys., A* **23**, 1775 (1990).

¹⁵C. Domb, in *Phase Transitions and Critical Phenomena*, edited by C. Domb and M.S. Green (Academic, New York, 1974), Vol. 3.

¹⁶A.J. Guttmann, in *Phase Transitions and Critical Phenomena*, edited by C. Domb and J. Lebowitz (Academic, New York, 1989), Vol. 13.